# NUMERICAL INVESTIGATION ON HOLLOW SECTION N-JOINTS MADE OF HIGH STRENGTH STEELS

PHILIPP LADENDORF[1] and THOMAS UMMENHOFER[1]

[1]*KIT Steel- and Lightweight Structures, Karlsruhe Institute of Technology, Karlsruhe 76131, Germany*
*philipp.ladendorf@kit.edu*

In this paper, the design capacity of a specific N-joint geometry with different yield strengths is compared with the numerical reaction forces of a single-joint-system and a truss-system by means of a finite element analysis in order to investigate the chord stress influence at the limit condition of chord plasticization failure (CPF). As basis, the design capacity for circular (CHS) and square hollow sections (SHS) according to EN 1993-1-8, CIDECT DG1 and DG3 is set as reference. Exemplary, the steel grades S235, S355, S460, S690 and S900 are chosen. The material parameters are derived from EN 10025-2 and -6 regarding $f_y$, $f_u$, as well as elongation at fracture A. For S900, the material data given by a hollow section manufacturer of hot rolled profiles has been chosen. As limit condition, a chord indentation of 3 % $b_0$ / $d_0$ resp. is evaluated. The reaction force at 3 % $b_0$ / $d_0$ of the vertical brace is compared with the design capacity at CPF. The results show, that both systems of SHS-N-joints are more critical than CHS-N-joints. For this specific joint, the design formulae seem to be applicable for CHS up to S900, considering the chord stress influence and the $C_f$-factors. The design formulae do not seem to be best suited for the SHS-geometry, whereas a $C_f$-factor of 0.7 could lead to an application of HSS SHS.

*Keywords*: high strength steels, hollow sections, N-joint, design capacity.

## 1 Introduction

During the last few years, hollow section manufacturers have made major progress in expanding high strength fine grain steel grades with yield strengths up to 900 MPa to hollow section profiles. In civil engineering however, not following this development, designers in Europe may not use high strength steels (HSS) above S700 due to regulatory reasons. In order to design buildings, engineers are obliged to use Eurocode 3 (EC3), which specifies the strength classes of steels up to S700 with reduction factors $C_f = 0.9$ for steels between S355 and S460, and $C_f = 0.8$ between S460 and S700 respectively. This accounts for less rotational capacity of HSS for hollow sections. The existing design formulae of EN 1993-1-8 are largely based on experimental investigations performed on steel grades with a yield strength up to 460 MPa and therefore, secondary effects are already included in the design formulae. In order to verify the formulae regarding sufficient rotational capacity of HSS above 460 MPa, the influence of yield and tensile strengths $f_y$, $f_u$ resp. and maximum uniform elongation $A_{gt}$ on the calculated design capacities of N-joints is investigated by means of a finite element analysis (FEA).

Within the scope of this numerical study, the existing design formulae for hollow section joints according to EN 1993-1-8 are compared with the CIDECT Design Guides 1 (Wardenier 2008) and 3 (Packer 2009). With respect to higher steel grades (in this case S690 and S900), the design formulae will be evaluated against the resulting strains of a finite element analysis for the common steel grades S235, S355 and S460. The investigation compares the results of a single-N-joint-model (cp. Figure 3) with a coupled beam-solid-model of a truss with ten spans (cp. Figure 4).

*Proceedings of the 17th International Symposium on Tubular Structures.*
*Editors:* X.D. Qian and Y.S. Choo

*Published by* Research Publishing, Singapore.
ISBN: 978-981-11-0745-0; doi:10.3850/978-981-11-0745-0_057-cd

## 2 Applicable material data from standard

For steel construction, table 3.1 of Eurocode 3, part 1-1 covers grades up to S460, whereas part 1-12 expands the applicable range up to S700. Other than this, the CIDECT Design Guides only allow yield strengths up to 460 N/mm². When using HSS hollow sections, both guidelines demand a compensation for the smaller amount of rotational capacity of HSS compared to S235 or S355 respectively. By applying EN 1993-1-8, all design resistances are calculated using the nominal yield strength $f_{y,nom}$. The calculated design resistance is then reduced by a correction factor $C_f = 0.9$ for 355 N/mm² < $f_{y,nom}$ ≤ 460 N/mm² and $C_f = 0.8$ for 460 N/mm² < $f_{y,nom}$ ≤ 700 N/mm² (cp. Table 1). The current CIDECT Design Guides use a modified design yield strength of $f_{y,mod} = \min(f_y ; 0.8\, f_u)$ to calculate the design resistances. The correction factor $C_f = 0.9$ also diminishes the resulting design resistance, but only for the covered steel grades with yield strengths 355 N/mm² < $f_{y,nom}$ ≤ 460 N/mm². Most likely, the current draft of prEN 1993-1-8 will also consider the usage of $f_{y,mod}$ combined with the reduction by $C_f$ for the calculation of the design resistances of HSS. While the application of this rule for S460 leads only to a reduction of the design capacity of about 15 %, the transfer to a yield strength up to 900 N/mm² can result in a loss of 32 % of the nominal yield strength. Figure 1 shows the reduction to $f_{y,mod}$ as a normalized yield strength related to S235. With this rule, it is not possible to use the full capacity of HSS with the current or future design formulae. All design resistances in this study are calculated using the method presented above, depending on the specific design guideline. This investigation uses the material parameters shown in Table 1.

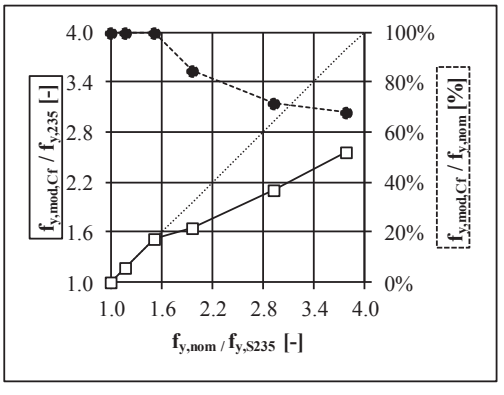


**Figure 1.** Ratios between $f_{y,mod}$ and $f_{y,nom}$

**Table 1.** Material data
[1] EN 1993-1-1, [2] EN 10025-6, [3] assumed, [4] data sheet manufacturer [5] only EN 1993-1-8

| Grade | $f_{y,nom}$ [N/mm²] | $f_u$ [N/mm²] | $f_{y,mod.}$ [N/mm²] | A [%] | $A_{gt}$[3] [%] | $C_f$ [-] |
|---|---|---|---|---|---|---|
| S235[1] | 235 | 360 | 235 | 26 | 16,0 | 1,0 |
| S355[1] | 355 | 510 | 355 | 22 | 10,0 | 1,0 |
| S460[1] | 460 | 560 | 414 | 17 | 7,5 | 0,9 |
| S690[2] | 690 | 770 | 552 | 14 | 5,0 | 0,8[5] |
| S900[4] | 900 | 960 | 768 | 14 | 3,5 | 0,8[3] |

## 3 Investigated geometry

The investigation uses N-joints in order to compare the established formulae of the above design codes with the numerical calculations for one of the most severe design cases due to high secondary bending moments. The cross sections' geometries consist of hot rolled circular and square hollow sections according to EN 10210. Figure 2 shows the selected dimensions for the joint geometries with outer radii of 1.5· $t_0$ and inner radii of $t_0$ for SHS. The numerical study uses butt welds without a specific weld geometry and without a distinction between filler and base material. The chosen geometry of the SHS lies slightly outside the valid parameter range of EN 1993-1-8 and DG3 regarding $2\gamma$ ($2\gamma_{act} = 14 < 15 = 2\gamma_{min}$).

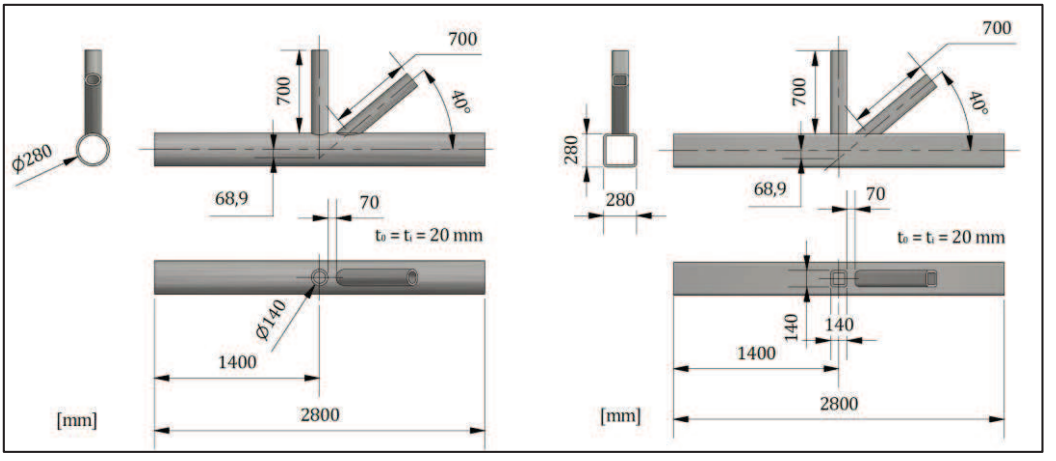


**Figure 2.** Selected geometry of CHS and SHS N-joints

## 4 Design capacities according to design codes

For CHS, chord plasticization failure (CPF) and chord punching shear failure (CPS) have to be investigated. For SHS, the design resistances against the failure modes CPF, CPS as well as brace failure (BF) and chord shear failure (CSF) have to be determined. In order to compare the standards, the chord stress function is neglected. The resulting resistances for CHS and SHS are presented in Table 2.

**Table 2.** Design resistance [kN] for CHS- and SHS-N-joint
*)currently not covered by existing design rules **)assumed

| CHS | EN 1993-1-8 (n = 0, $f_{y,nom}$) | | | | | CIDECT DG1 (n = 0, $f_{y,mod}$) | | | | |
|---|---|---|---|---|---|---|---|---|---|---|
| | **S235** $C_f = 1,0$ | **S355** $C_f = 1,0$ | **S460** $C_f = 0,9$ | **S690** $C_f = 0,8$ | **S900*** $C_f = 0,8^{**)}$ | **S235** $C_f = 1,0$ | **S355** $C_f = 1,0$ | **S460** $C_f = 0,9$ | **S690*** $C_f = 0,8^{**)}$ | **S900*** $C_f = 0,8^{**)}$ |
| CPF | 1023 | 1545 | 1801 | 2402 | 3133 | 1270 | 1918 | 2179 | 2663 | 3320 |
| CPS | 1193 | 1803 | 2103 | 2803 | 3657 | 1199 | 1811 | 2057 | 2514 | 3135 |
| **SHS** | **EN 1993-1-8 (n = 0, $f_{y,nom}$)** | | | | | **CIDECT DG3 (n = 0, $f_{y,mod}$)** | | | | |
| CPF | 1107 | 1672 | 1950 | 2600 | 3391 | 1180 | 1782 | 2024 | 2474 | 3084 |
| BF | 2068 | 3124 | 3643 | 4858 | 6336 | 2534 | 3124 | 3548 | 4337 | 5407 |
| CPS | 1411 | 2132 | 2486 | 3314 | 4323 | 1737 | 2141 | 2702 | 3716 | 4633 |
| CS | 1702 | 2571 | 2999 | 3998 | 5215 | 1710 | 2583 | 2934 | 3586 | 4470 |

Neglecting the chord stress function, the capacity for chord punching shear is governing the failure mode, when calculating the resistance acc. to DG1. The difference between CPF and CPS in design resistance is below six percent. Since the calculation of punching shear failure is only possible by considering damage functions, the chord plasticization failure is the basis for the comparison between the standards and the FEA. For the SHS-N-joint, the design capacity for CPF is governing the remaining failure modes.

## 5 Numerical investigation

The basis for the comparison of the existing design formulae with the FEA consists of two approaches. The first approach uses a single joint system with one free end to be able to set the chord stress to n = 0 below the compression brace (Figure 3). The second approach embeds the isolated single joint into a truss system to be able to consider the chord stress influence, which increases gradually with growing displacement (Figure 4).

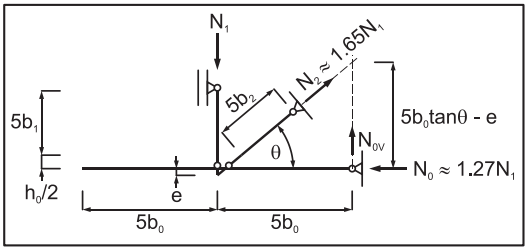


**Figure 3.** Loading condition of single joint system, (Ladendorf et. al, 2018)

The numerical investigation uses ANSYS 2019 R1. For the single joint system, the profiles' open ends have been coupled with the reference points using constraint points as pinned supports. The load has been applied as axial displacement at the vertical compression brace. The discretization has been established by using a reduced integrated, structural hexahedral mesh with five layers of quadratic volume elements (SOLID186) in the vicinity of areas with large plastic deformations. A symmetry boundary condition has been applied in order to reduce computational time. The meshed FE-model is shown in Figure 6. In order to fulfill the requirements of a truss, the dimensions have been chosen to fit into $12 < L / H < 15$. To compare the single joint system and the truss system, each span of the truss has a length of 2.8 m. By assuming 10 spans, the overall length is 28 m. The height is chosen to be 2.2 m. The load is applied as axial displacement $\delta$ above the compression brace. Kinematic couplings establish the connection between the solid elements of the joint and the bars of the remaining truss. All bar elements are rigidly connected without considering pin joints. The FEA is carried out on a full expansion 3D model without the use of symmetry boundary conditions.

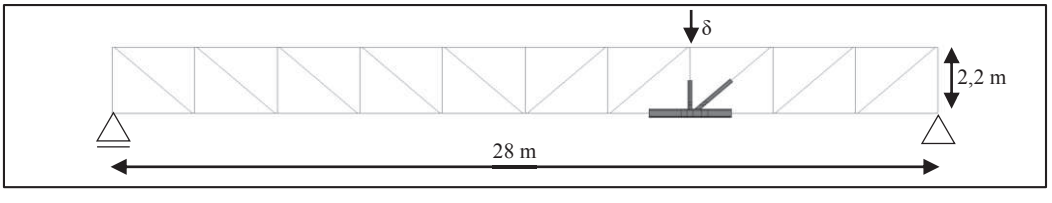


**Figure 4.** Truss system and loading condition

The conversion of $f_y$, $f_u$ and $A_{gt}$ as engineering stresses and strains into true stresses and strains is performed by using Eq. (1) and Eq. (2). Young's modulus is set to 210 000 N/mm² and Poisson's ratio to $\nu = 0.3$. After reaching $A_{gt}$, the stress remains constant at a plateau defined by $f_u$. The determined joint capacity is based on the 3 % chord indentation criterion. The reaction force $R_1$ is extracted at a chord indentation of $\delta_1 = 0.03 \cdot d_0 = 8.4\ mm$ or $\delta_1 = 0.03 \cdot b_0 = 8.4\ mm$ resp. (Lu et al., 1994). Figure 5 shows the geometric locations for the determination of the chord indentation for CHS and SHS. $\delta_1$ is always calculated as vertical distance between the two indicated points.

$$\sigma_{true} = \left(1 + \varepsilon_{eng}\right) \cdot \sigma_{eng} \tag{1}$$

$$\varepsilon_{true} = \ln\left(1 + \varepsilon_{eng}\right) \tag{2}$$

Figure 7 and Figure 8 show the resulting load-indentation curves of both section types for the investigated mechanical properties according to Table 1. While the black curves show the

results of the single joint system, the grey curves represent the truss system. Both figures additionally show the indicated 8.4 mm displacement criterion in order to compare the different yield strengths with each other. Table 3 summarizes the results of the linear interpolation between the data points of the FEA and shows the scaling factor $S_F$ (Liu et. al, 2004) for the different steel grades, based on the 3 % indentation criterion for S235 according to Eq. (3). Table 3 also contains the chord stress ratio n on the left-hand side of the joint, resulting from the FEA, as well as the design resistance from DG1/3 and the corresponding reaction force $R_1$.

$$S_F = \frac{N_{\text{ultimate,S...}}}{N_{\text{ultimate,S235}}} \cdot \frac{f_y(\text{S235})}{f_y(\text{S...})} \tag{3}$$

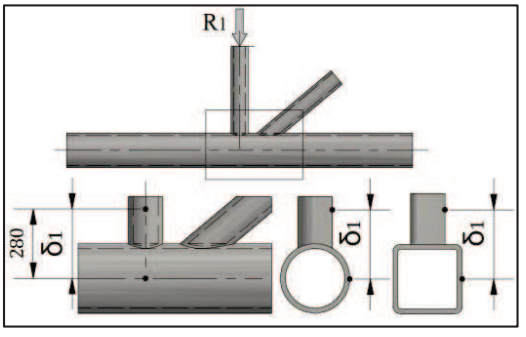


**Figure 5:** Location of $\boldsymbol{\delta_1}$ CHS and SHS

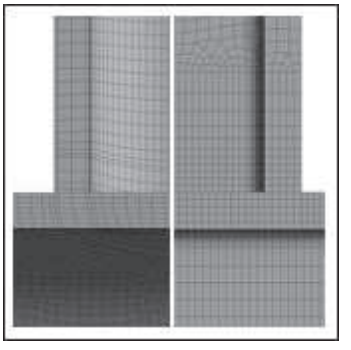

**Figure 6:** Discretization below compression brace CHS (left) and SHS (right)

The difference of the resulting reaction forces $R_1$ between the CHS single joint and the truss system is bigger than the difference between the SHS systems. The chord stress effect does not seem to have such a big impact on the resulting reaction force for the SHS systems compared to the CHS systems.

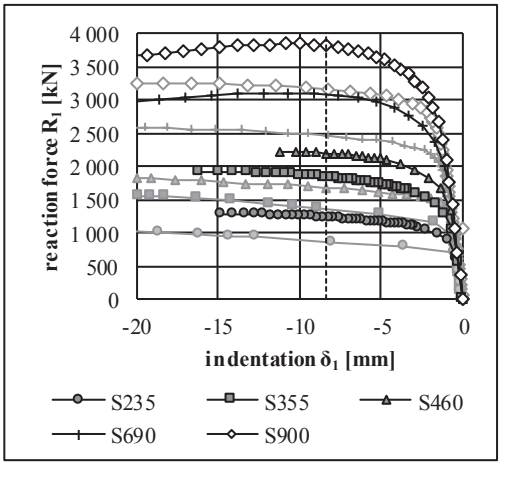


**Figure 7:** Load-indentation curves CHS, single joint (black) and truss systems (grey)

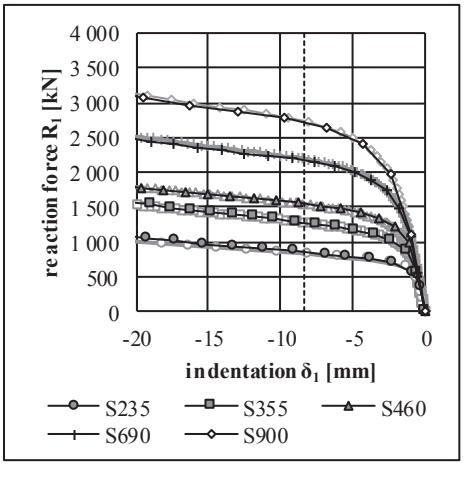


**Figure 8:** Load-indentation curves SHS, single joint (black) and truss systems (grey)

Figure 9 and Figure 10 show the calculated design resistances of the single-joint (empty circles and squares) and truss systems (filled circles and squares) for CHS and SHS normalized to

the design resistances of the corresponding design codes in conjunction with the particular assumptions regarding $C_f$ (dotted lines above $f_y$ = 460 N/mm²). Above the horizontal line, the ratio shows a conservative and below, an optimistic result regarding the design value.

For the CHS-single-joint, the reaction force $R_1$ at 3 % chord indentation correlates well with the calculated design resistance up to $f_y$ = 460 N/mm² for DG1, whereas EN 1993-1-8 is on the conservative side. Since the design formulae of EN 1993-1-8 and DG3 result in similar values for the SHS-single-joint, both design guidelines overestimate the design capacity considering n = 0.

**Table 3:** Reaction forces $R_1$ [kN], scaling factors $S_F$, chord stress ration n and design resistance with respect to chord stress [kN] of the investigated systems
*)assumed

| Grade | CHS | | | | | | SHS | | | | | | $C_f$ |
|---|---|---|---|---|---|---|---|---|---|---|---|---|---|
| | $R_{1,S.J.}$ | $S_{F,S.J.}$ | $R_{1,Tr.}$ | n | DG1, n = X | $S_{F,Tr.}$ | $R_{1,S.J.}$ | $S_{F,S.J.}$ | $R_{1,Tr.}$ | n | DG3, n = X | $S_{F,Tr.}$ | |
| S235 | 1223 | 1.00 | 875 | 0.78 | 940 | 1.00 | 975 | 1.00 | 825 | 0.74 | 1045 | 1.00 | 1.0 |
| S355 | 1833 | 0.99 | 1355 | 0.74 | 1466 | 1.02 | 1370 | 0.93 | 1260 | 0.68 | 1592 | 1.01 | 1.0 |
| S460 | 2204 | 0.92 | 1680 | 0.83 | 1536 | 0.98 | 1660 | 0.87 | 1543 | 0.60 | 1848 | 0.96 | 0.9 |
| S690 | 3088 | 0.86 | 2465 | 0.79 | 1947 | 0.96 | 2170 | 0.76 | 2193 | 0.54 | 2287 | 0.91 | 0.8 |
| S900 | 3823 | 0.82 | 3172 | 0.77 | 2481 | 0.95 | 2714 | 0.73 | 2734 | 0.56 | 2841 | 0.87 | 0.8* |

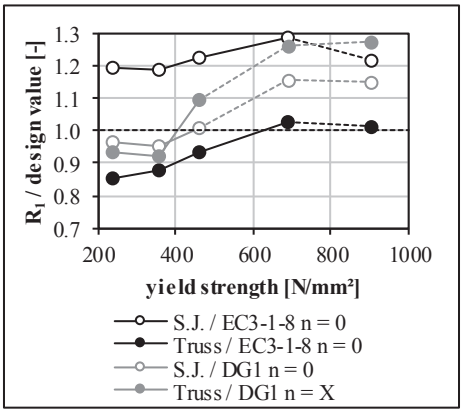


**Figure 9.** CHS, $R_1$ normalized vs. design values

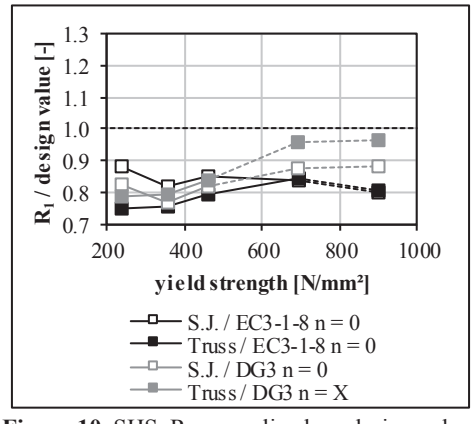


**Figure 10.** SHS, $R_1$ normalized vs. design values

The current version of EN 1993-1-8 neglects the chord stress function for chords in tension. The Design Guides 1 and 3 aim to consider this effect by reducing the design capacity by a reduction function $Q_f$. For all investigated configurations, the chord stress at 3 % chord indentation is the basis of the calculation of the corresponding function $Q_f$ to derive the modified joint capacity. While the design capacities of EN 1993-1-8 correlate quite well with the FEA-results for the CHS-truss-system in S690 and S900, DG1 is on the conservative side. For the SHS-truss-system, both design codes overestimate the capacities for this specific N-joint geometry. Even though DG3 uses a modified yield strength $f_{y,mod}$ to calculate the design resistances, the results of the 3 % chord indentation lie below the horizontal line.

Figure 11 shows the scaling factor R derived by Eq. (3) and the corresponding results of the FEA as well as the normative and assumed correction factor $C_f$. For the investigated, specific type of single-N-joint, the established $C_f$-Factor from the standards is conservative for CHS, but optimistic for SHS. By scaling the higher strength truss-systems to the level of the S235 truss-system, a different conclusion can be drawn. For all yield strengths, the $C_f$-factor seems to be conservative. This evaluation shows that the scaling factor does not only depend on the yield

strength or the type of profile but also on the level of chord stress. While the chord stress is set to zero in the single joint, it is immanently included in the truss system. In case the chord stress ratio for S235 is high, the resulting scaling factor for grades with lower stress ratios is optimistic. Nevertheless, the decreasing scaling factors show, that higher yield strengths combined with higher $f_y/f_u$ ratios lead to smaller design capacities in direct comparison with the 3 % resistances of the grade S235.

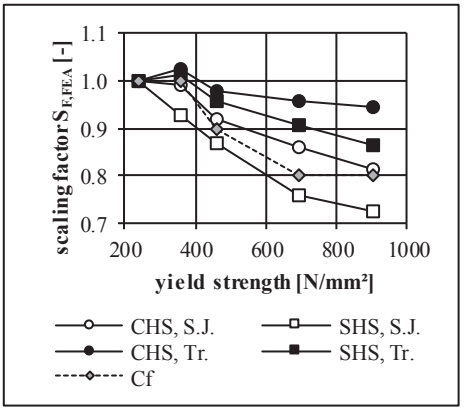


**Figure 11.** Comparison of $S_{F,FEA}$ and $C_f$

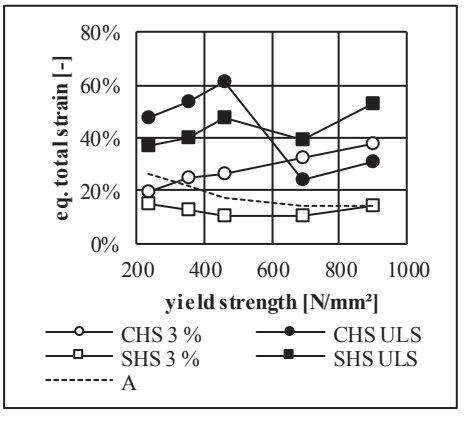


**Figure 12.** Strains at 3 % and ULS, Truss

When comparing the investigated steel grades, the question arises, if the normative uniaxial elongation at fracture A could be exceeded, when the reaction force $R_{ULS}$ reaches the design capacity. Figure 12 contains the equivalent total strains for the CHS and SHS truss systems at 3 % chord indentation at ultimate limit state (ULS), which is characterized by the design capacity of EN 1993-1-8. The locations of the maximum strains for SHS vary between the inside of the upper chord face below the compression brace and the connection between chord and tension brace in the gap area (cp. Figure 13 and Figure 14). For the CHS truss system, the maximum strains occur directly at the intersection between compression brace and chord. Due to a significant element distortion at this specific point, the CHS system is evaluated at the same location as SHS. Since the 3 % reaction force $R_1$ for S690 and S900 is above the design capacity acc. to EN 1993-1-8, the strains for both grades at ULS are below the strains of the 3 % criterion. Besides the CHS-truss-system in S235 and the 3 %-$R_1$ for SHS, the resulting strains exceed the uniaxial elongation at break A. Further investigations are necessary to implement damage functions like the GTN-model based on normative material properties (Feldmann et al., 2015) in order to obtain reliable results, after the actual strains surpass $A_{gt}$.

By comparing the results of the FEA to the design codes, CHS do not seem to be as critical as SHS, if the underlying assumption of the 3 % criterion is set as reference. If the chord stress function $Q_f$ is taken into consideration, even the CHS-Truss system of S690 and S900 seem to be covered by the CIDECT Design Guide 1 by assuming a factor of $C_f = 0.8$. The formulae for SHS do not seem to be best suited for this specific N-joint-geometry, due to the fact, that both the single joint and the truss system deliver results below the design resistances derived by EN 1993-1-8 and DG3. Although the design resistances of DG3 are within a span of 5 % of the 3 % reaction force for S690 and S900, the remaining grades defer up to 20 %. For S690 and S900, a factor as low as $C_f = 0.7$ should be taken when applying the rules of DG3 to this this specific N-joint.

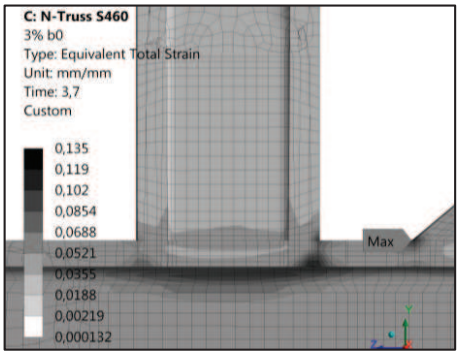


**Figure 13.** Maximum strains at tension brace

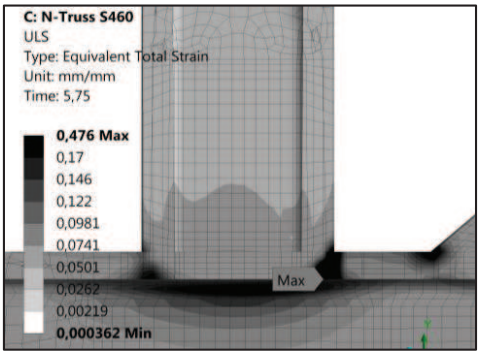


**Figure 14.** Maximum strains below compr. brace

## 6 Conclusion

The present paper investigates the influence of different yield strengths $f_y$, tensile strengths $f_u$ and uniform elongations $A_{gt}$ on the resulting design capacities derived by the 3 % chord indentation criterion for hot rolled circular and square hollow section-N-joints. The results of the FEA show, that the 3 % chord indentation criterion delivers results below the design capacities calculated by the design formulae of EN 1993-1-8 and DG1/3. If the resulting equivalent total strains are compared with the uniaxial elongation at fracture A, the results show lower strains when reaching 3 % chord indentation, but larger strains when reaching the reaction force $R_1$ at ULS. While this investigation only uses an assumption for the uniform elongation $A_{gt}$, the results might be slightly optimistic compared to the usage of the uniform elongation at fracture A (Lu, 1994). Because of the fact, that both simplifications do not account for any damage function, further investigations should consider damage functions, for example the GTN-parameters in order to represent a proper joint behavior after reaching $f_u$. For CHS, a factor of $C_f = 0.8$ seems to be applicable for the steel grades S690 and S900 with the specific N-joint geometry and the underlying material assumptions. For this specific SHS-N-joint, a factor $C_f = 0.7$ could lead to an application of HSS for SHS.

## References

EN 1993-1-1, Eurocode 3: Design of steel structures - Part 1-1: General rules and rules for buildings

EN 1993-1-12, Eurocode 3: Design of steel structures - Part 1-12: Additional rules for the extension of EN 1993 up to steel grades S700

EN 1993-1-8, Eurocode 3: Design of steel structures - Part 1-8: Design of joints

Feldmann, M., Schaffrath, S.: Duktilitäts- und Zähigkeitsanforderungen für hochfeste Stähle bei festigkeitsgesteuertem Versagen. Stahlbau 84, S. 682-688, 2015

Ladendorf, P., Ummenhofer, T., Fleischer, O., Hollow Section N-joints made of High Strength Steels, First Workshop on High Performance Steel Structures Research Council (HPSSRC), May 15-16, 2018, Delft

Liu, D.K., Wardenier, J., Effect of the yield strength on the static strength of uniplanar K-joints in RHS (steel grades S460, S355 and S235) IIW Doc. XVE-04-293, 2004

Lu, L.H., de Winkel, G.D., Yu, Y., Wardenier, J., Deformation limit for the ultimate strength of hollow section joints, Tubular Structures VI, Grundy, Holgate & Wong (eds.), Balkema, Rotterdam, 1994

Packer, J.A., Design guide for rectangular hollow section (RHS) joints under predominantly static loading, second edition, CIDECT, 2009

Wardenier, J., Design Guide for circular hollow section (CHS) under predominantly static loading, second edition, CIDECT, 2008